# SAGE II measurements of stratospheric aerosol properties at non-volcanic levels

**L. W. Thomason,[1] S. P. Burton,[2] Bei-Ping Luo[3], and Thomas Peter[3]**

[1]{NASA Langley Research Center, Hampton, Virginia}
[2]{Science Applications International Corporation, Hampton, Virginia}
[3]{Institute for Atmospheric and Climate Science, Zurich, Switzerland}

## Abstract

Since 2000, stratospheric aerosol levels have been relatively stable and at the lowest levels observed in the historical record. Given the challenges of making satellite measurements of aerosol properties at these levels, we have performed a study of the sensitivity of the product to the major components of the processing algorithm used in the production of SAGE II aerosol extinction measurements and the retrieval process that produces the operational surface area density (SAD) product. We find that the aerosol extinction measurements, particularly at 1020 nm, remain robust and reliable at the observed aerosol levels. On the other hand, during background periods, the SAD operational product has an uncertainty of at least a factor of 2 during due to the lack of sensitivity to particles with radii less than 100 nm.

## 1 Introduction

SAGE II (Stratospheric Aerosol and Gas Experiment) operated in low Earth orbit between October 1984 and August 2005 producing globally distributed profiles of ozone, $NO_2$, water vapor, and aerosol extinction at four wavelengths from the middle troposphere though the stratosphere. It is the third in a series of four solar occultation instruments whose records begin in 1978 and ended in March 2006. During this time the variability of aerosol in the stratosphere was dominated by a series of large volcanic perturbations and followed by multi-year recoveries. The most significant of these eruptions are El Chichon, which occurred in 1982 but persisted into the SAGE II observational period, and the June 1991 Pinatubo eruption. The latter eruption was the most stratospherically significant volcanic event of the past 30 years and was responsible

for significant radiative and chemical effects in the atmosphere (e.g., McCormick et al., 1995). The SAGE II data also records perturbations associated with a number of smaller volcanic events including the eruptions of Nevado del Ruiz/Nyamuragira (1985/1986), Kelut (1990), Cerro Hudson (1991), and Ruang/Reventador (2002). For most of the SAGE II record, the stratosphere can be considered to be in recovery from volcanic perturbations.

The 1979-2004 multi-instrument 1000-nm stratospheric optical depth is shown in Figure 1. The stratospheric column optical depth was well in excess of 0.1 following the eruption of Pinatubo. However, in recent years, the lack of stratospherically significant volcanic activity has led to the lowest optical depth values in the 28-year record with minimum values near 0.001 or a factor of more than 100 smaller than the maximum. At some altitudes, changes in the measured aerosol extinction have varied by a factor in excess of 1000. Immediately following Pinatubo, the aerosol extinction profiles often terminated well above the tropopause. As a result, the optical depths between the eruption and mid 1993 are computed by extrapolating the profiles from the bottom of the profile down to the tropopause using the method used in the SPARC Assessment of Stratospheric Aerosol Properties (Thomason and Peter, 2006). The premature termination of profiles is commonly referred to as the 'saturation' effect that represents the upper bounds of the SAGE II dynamic range and occurs when the line of sight optical depth observed by the instrument (through the limb of the Earth's atmosphere) exceeds measurable bounds (a value of about 7). Saturation, due to Pinatubo effects, occurs from shortly after the eruption through mid-1993. It additionally occurs throughout the SAGE II record due to the presence of clouds, though mostly in the troposphere. In fact, clouds in the troposphere are the most common mechanism for defining the lower altitude extent of extinction profiles.

Since 2000, aerosol extinction has been characterized by relatively steady levels throughout the stratosphere and may represent a non-volcanically perturbed stratosphere. With the exception of a minor perturbation by the eruptions of Ruang and Reventador in late 2002, this is by far the longest period of steady aerosol levels in satellite measurement era and is the first such period occurring since the late 1970's. This extended period represents an opportunity to observe the optical manifestations of the

non-volcanic processes that control stratospheric aerosol under these conditions including possible human-derived effects. For instance, Figure 2 shows the aerosol extinction at in the tropics at altitudes between 18 and 30 km. The SAGE II extinction record at these altitudes show a significant annual cycle at 18 km whose source is not immediately obvious though it is at least in part due to temperature and water vapor variations. There is also a significant aerosol variability that appears to have a period similar to the Quasi-Biennial Oscillation (QBO) at 30 km. The extinction measurements generally show virtually no annual or QBO cycles at 22 or 26 km.

With aerosol at such low levels, it is fair, as a corollary to the saturation problem, to ascertain the degree to which SAGE II extinction measurements remain dependable at the reported levels and, by extension, determine whether measurement features like the tropical annual aerosol extinction cycle are robust features of aerosol morphology. Several factors may influence the robustness of the measurements at low levels. These include measurement noise, removing the effects of molecular scattering and absorption by ozone and nitrogen dioxide, dark current subtraction, and altitude registration. Herein, we discuss the sensitivity of the product to the major components of the processing algorithm used in the production of SAGE II aerosol extinction measurements. In addition to extinction, SAGE II provides an estimate of the aerosol surface area density (SAD) as an operational product (Thomason et al., 1997). Since visible and near-infrared wavelength aerosol extinction is insensitive to particles with radii smaller than 100 nm, the robustness of SAD estimates based on these measurements is questionable. Therefore, we have also included a study of the limitations of SAD estimates based on SAGE II aerosol extinction measurements.

## 2 SAGE II Aerosol Extinction Measurement Sensitivity Study

### 2.1 An overview of the retrieval process

SAGE II is a solar occultation instrument. It records the attenuation of sunlight by the Earth's atmosphere at seven wavelengths between 386 nm and 1020 nm during each sunrise and sunset encountered by the spacecraft. As the sun rises or sets, the instrument scans across the face of the sun, thereby obtaining multiple measurements of total slant

path transmittance for a given ray tangent altitude. Since measurements are also made for ray paths outside the atmosphere, this technique is self-calibrating. The tangent altitude of each ray path is calculated from spacecraft and sun ephemeris data, taking into account the shape of the Earth and atmospheric refraction. The total slant path optical depth data are corrected for molecular scattering using meteorological data from the National Centers for Environmental Prediction (NCEP) supplemented with climatological data at higher altitudes. Then the information for the seven SAGE II channels is separated into slant path optical depth contributions for ozone, nitrogen dioxide and water vapor plus aerosol in four channels (centered at 1020 nm, 525 nm, 452 nm and 386 nm) using a least squares technique in which aerosol effects at 448, 600, and 945 nm are estimated using a physically-based interpolation from the other channels. Finally, the slant path profiles undergo vertical inversion to produce vertical profiles of aerosol extinction in four channels, ozone and $NO_2$ number density, and $H_2O$ mixing ratio (e.g., Chu et al., 1989). For the sensitivity study, we will show results based on events occurring between 10 and 30°N during the extended low aerosol loading period. This latitude band was chosen because column aerosol loading is relatively low in this region (see Figure 1) and therefore potentially the most difficult region in which to make aerosol measurements though the following results are generally applicable to all latitudes.

### 2.2 Sensitivity study

The raw measurement obtained by the instrument is solar power as an integer number of counts from 3 or 4 (off-sun) to a few thousand, depending on the channel. The values measured through the Earth's limb are normalized by the exoatmospheric counts to generate transmittance measurements. The peak exoatmospheric count levels have generally decreased slowly over the lifetime of the instrument. Figure 3 shows the peak exoatmospheric count levels for the center of the Sun for the seven spectral channels from 1984 to 2005. Since the electronic noise level for the instrument is very low (less than one count), the signal-to-noise ratio for this data is very high. However, as the instrument scans from edge to edge across the face of the sun, the number of counts decreases toward zero, so only data from the center 90% of the Sun is used to compute transmission. Count levels also decrease as the path through the atmosphere approaches

the Earth's surface. Figure 4 shows the raw counts measured in the 1020 nm channel as a function of altitude for a single event in December 2003 and demonstrates that the bulk of the on-sun measurements in the stratosphere and well into the troposphere have count levels of 1500 or higher.

The transmittance signal in each channel is attributable to multiple sources: aerosol and molecular scattering and absorption by ozone, $NO_2$, and water vapor. Specifically, the aerosol extinction signal in the 1020 nm channel must be separated from the signal due to molecular scattering plus a small contribution from ozone absorption. Figure 5 shows the fraction of the signal in the 1020 nm channel due to aerosol. This fraction varies from about 40% to 60% below 30 km showing that 1020-nm extinction is not sensitive to the removal of interfering species.

Other parameters besides the sensitivity to aerosol could potentially handicap the aerosol measurements, including a number of possible sources of bias hinted at in the description of the retrieval above. The aim of the sensitivity study is to examine the effect on 1020 nm and 525-nm aerosol extinction data of various sources of systematic error, including the dark (off-sun) measurement, the altitude registration, the meteorological input data, and the gas cross-sections. In the following discussion, we demonstrate that the 1020-nm aerosol extinction is not sensitive to any of these sources while the 525-nm aerosol extinction is sensitive only to the ozone cross-section.

### 2.2.1 Dark Count Subtraction

The dark count value is measured by pointing the instrument away from the sun and represents the instrument's 'zero' level. In processing, this value is subtracted from the raw solar power measurements before the calibration by the exoatmospheric scans is performed. The seven dark count values are all between 3 and 4 counts, or about one or two one-thousandths of the maximum intensity measured. Over the lifetime of the instrument, dark count values have been stable for each measurement channel. Ironically, the generally desirable characteristics of very small measurement noise and a high stability of the dark count level conspire to make precise measurements of dark counts

difficult. Our confidence is near a half count and therefore is a large fraction of the overall dark count value.

In practice, dark count subtraction will have its greatest impact when the channels are near saturation and the measured total count level is close to the background value. In the stratosphere, this only occurs immediately after the Pinatubo eruption in 1991. In stratospheric background periods it occurs only in the presence of clouds for the 1020-nm channel and for clouds and in clear skies at and below ~6 km for the 525-nm channel. In order to determine the sensitivity of the aerosol measurements to the uncertainty in the dark count subtraction, we performed two experiments in which the magnitude of the dark count subtraction was changed by one count, first in the 1020 nm channel and then in the 525 nm channel. Figure 6 shows the results of these experiments on the ratio of detected aerosol extinction (525 nm/1020 nm). The events were 25 subtropical events from December 2003. They were reprocessed with a change in the dark count subtraction of one count. The resulting systematic change when the assumed background is changed in the 1020-nm channel is a fraction of a percent. The effect of adjusting the 525-nm background is slightly larger, but is still less than a percent below 30 km, except in the vicinity of 15 km where it is about 2% in the 525-nm extinction (visible here as a similar change in the ratio, since the change in 1020-nm extinction is near zero). As expected, we find that background stratospheric aerosol measurements are not greatly influenced by the dark count subtraction.

### 2.2.2 Altitude registration sensitivity

The determination of the ray tangent altitude is another potential source of systematic error. In a similar experiment to that described above, the altitude registrations were artificially shifted upward and downward by 100 m. This shift is comparable to the altitude registration uncertainty derived from ozone intercomparisons [e.g., Wang et al., 2002]. The shift was experimentally applied to all profiles in the 10º-30º N latitude band in October 2001 through September 2002. The result, shown in Figure 7 shows that the effect on 1020 nm aerosol extinction is less than 3% throughout the stratosphere. The effect of an upward (downward) shift on the 525-nm aerosol measurement is to decrease

(increase) the inferred extinction by about 2-5% almost everywhere in the stratosphere, with the peak shift near 31-33 km. Even at the peak value, where the difference is 6% in the measured 525-nm aerosol extinction and the 525 to 1020-nm extinction ratio, the systematic error resulting from this experiment is quite small.

### 2.2.3 Temperature profile sensitivity

In our third experiment, we examine the effect on the SAGE II aerosol extinction measurements of an artificially induced systematic bias in the NCEP temperature profiles at the 100 mb level. Randel et al. [2000] has reported that the NCEP tropopause temperature is too warm by approximately 3-5 K. The possibility of a systematic error or a spurious trend in the temperature data is of particular concern to SAGE II measurements since such an error can produce a bias or an artificial trend in the aerosol measurements. Accordingly, we have experimentally adjusted the temperature profiles that are input to the SAGE II retrieval for the same 10º-30º N latitude band in October 2001 through September 2002. The 100 hPa level occurs at approximately the same altitude as the tropopause but it is not unreasonable to anticipate that a possible change in the temperature profile at one point could affect higher altitudes.

First, the temperature at the 100 hPa level was increased by 3 K. The result is an increase of 9% in a narrow region near 16 km and a decrease of generally less than 1% in the 525-nm channel in the stratosphere (Figure 8, top middle). In the 1020-nm channel, the narrow peak is somewhat smaller, while stratospheric values again change by 1% or less (Figure 8, top left). As expected, decreasing the temperature results in equivalent changes opposite in sign to those described above (Figure 8, bottom left, middle, and right).

The temperature uncertainty at a lower pressure level (higher altitude) may be more relevant to stratospheric aerosol measurements. Therefore, in a separate experiment, we have tested the response of the aerosol measurements to an increase or decrease of 3 K in the 10 hPa level (about 31 km). This is close to where an annual cycle of about 50% is seen in SAGE II aerosol measurements. Figure 8 also demonstrates the response of the aerosol extinction measurements to this perturbation. Increasing the temperature

produces an increase in the measured 1020-nm aerosol extinction between 25 and 38 km, with a peak effect of about 4% near 34 km. The effect on the 525-nm measurement is increasing between about 25 and 31 km, with a peak of about 5% at 29.5 km, and a constant decrease of about 2% above 31 km. Decreasing the temperature produces approximately opposite effects, as expected.

### 2.2.4 Sensitivity to mirror correction

In an additional experiment, we assess the effect of a theoretical bias in the mirror correction. This small correction that is nearly linear with altitude that is made to correct for variation in the mirror reflectivity as a function of the mirror angle. The correction is small through out the depth of the atmosphere and never exceeds 1% with an estimated relative uncertainty of 0.4%. While the expected effect was expected to be quite small, we tested the effect of the mirror correction on the aerosol extinction profiles by making the mirror correction by one sigma (0.4%) larger than the operational values. The effect on the 525-nm and 1020-nm aerosol extinction profiles is negligible throughout the 15-35 km region, with a maximum effect of only 1.8% near 38 km in the 1020-nm channel and less than 1% at 34 km in the 525-nm channel. These effects are very small and only occur at the high altitude extreme of the aerosol profiles where measurement uncertainty is already close to 100%.

### 2.2.5 Sensitivity to aerosol model

The SAGE II species retrieval includes an aerosol model which is used to calculate the aerosol extinction in the 600-nm channel where it is an interfering species in the ozone retrieval. The calculation estimates the aerosol slant path optical depth as a linear combination of the aerosol optical depth in the 1020-nm and 525-nm channels. The model, similar to that described by Chu et al. (1989), is based on the relationship between 525 and 1020-nm extinction with that at 600 nm as defined by a family of log-normal aerosol size distributions that are representative of stratospheric aerosol. The model is estimated to produce 600-nm aerosol extinction estimates with an accuracy of ~1%. Following this, we perturbed the 600-nm aerosol by changing the coefficients multiplying

the other two channels, both separately and together, by one percent. Since the retrieval is a simultaneous retrieval of the gaseous species and aerosol in all channels, there is potential crosstalk between the retrieval of ozone and aerosol extinction, particularly for the shorter wavelength aerosol channels, through the aerosol model. However, we find that these perturbations have a negligible effect on the 1020-nm and 525-nm aerosol extinction. The effect on the 1020-nm aerosol extinction was effectively zero (less than 0.01%) in all three tests; the maximum effect on the 525-nm aerosol extinction was less than four tenths of a percent (this occurred when both coefficients were simultaneously biased away from their standard values in the same sense).

### 2.2.6 Ozone cross-section sensitivity

The final component of the sensitivity study is an assessment of the effect of a systematic error in the ozone cross-section. SAGE II version 6.2 uses the ozone cross sections of Anderson and Mauersberger (1992) and Anderson et al. (1990, 1991, 1993a, 1993b) and the temperature dependence measured by Burkholder and Talukdar (1994), as compiled by Shettle and Anderson (1994). These cross sections report an uncertainty of 1-2% and a temperature dependence of less than 1% at stratospheric temperatures near the peak of the Chappuis band and of about 5% near 525 nm. Ozone absorption cross-sections for each channel are required the retrieval of individual species. These are derived by combining the above cross sections with the SAGE II instrument's filter response function. Since the 525-nm channel is within the Chappuis band, the cross section at that channel is a potential source of systematic error in the aerosol measurements. However, the ozone cross section at 1020 nm is very small and unlikely to play a role in the aerosol extinction coefficient measurement quality. The test consists of a perturbation of 1% in the ozone cross section for that the 525-nm channel. Figure 9 shows that, predictably, there is almost no effect on the 1020 nm aerosol extinction, but a significant effect on 525 nm aerosol extinction that increases with altitude reaching 18% at 31 km. A related experiment was also performed in which the cross section for the primary ozone channel (at 600 nm) was also changed by 1%. The effect on the 525-nm aerosol extinction measurement is in the opposite sense than the previous experiment but with a similar

altitude dependence. The peak change is about 20% near 33 km. The effect on the 1020 nm aerosol extinction measurement is again nearly zero.

As a result, we find that a systematic bias in the ozone cross section (either in an absolute sense or in its temperature dependence) could produce artificial seasonal cycles in the inferred aerosol extinction coefficient variability but only at the short wavelength channels like 525 nm. The 1020-nm channel is essentially independent of ozone cross section errors and therefore, annual cycles in aerosol that appear in both the short wavelength channels and the 1020-nm are likely to reflect real changes in the aerosol morphology rather than a residual ozone signature. This includes the annual cycles (shown Figure 2) in the tropical lower stratosphere (amplitude ~20%) and the annual cycle near 30 km where the amplitude is near 50%. It also implies that the real uncertainty in the 525-nm ozone cross section must be significantly less than 1%.

### 2.3 Summary of Aerosol Extinction Coefficient Sensitivity Study

We find that during the low aerosol levels found in the stratosphere beginning in 2000 and continuing through the end of its mission 2005 SAGE II aerosol extinction coefficient profiles remained robust and reliable. While the relative uncertainty associated with measurement noise were larger than higher aerosol loading periods, the potential for significant measurement bias remained low. For these conditions, at 1020-nm, the maximum bias is less than 5% from the tropopause to 30 km and is dominated by the potential for bias in the a priori temperature profile data used in the data processing. At 525 nm, the potential for bias is less than 10% through most of the lower stratosphere and approaches 20% at 30 km. In this case, the bias potential is dominated by uncertainty in the temperature profile data and in the ozone cross section.

## 3. Surface Area Density Estimation Sensitivity

### 3.1 A Model for Determining the Limiting Bounds on SAD

The operational SAGE II data processing includes estimated surface area density (SAD) beginning with the release of Version 6.2. The method employed follows that described by Thomason et al. (1997) except the coefficients used in the operational retrieval are weighted by measurement uncertainty that moves the SAD derivation dependence toward the 525 and 1020-nm channels rather than the short wavelength channels that are generally less reliable. Operationally, this approach was simplified to this expression

$$SAD = k_{1020}\left(\frac{1854.97 + 90.137 * r + 66.97 * r * r}{1. - 0.1745 * r + 0.00858 * r * r}\right) \quad (1)$$

where $r$ is the 525 to 1020-nm aerosol extinction ratio, and $k_{1020}$ is the 1020-nm aerosol extinction coefficient in units of $km^{-1}$ and the equation yields surface area density in units of $\mu m^2\, cm^{-3}$. This technique was shown to produce values comparable with those produced by in situ instruments such as the University of Wyoming Optical Particle Counter (OPC) during the post-Pinatubo period (e.g., Thomason et al., 1997) but more recent work shows that it tends to underestimate OPC-derived SAD during low aerosol loading periods such as the current period (e.g., Thomason and Peter, 2006). It is not surprising that SAD calculations based on visible wavelength extinction measurements are less robust during low aerosol periods since the inferred aerosol properties like SAD become increasingly dependent on particles smaller than 100 nm which are rather poor scatterers and thus have only a small impact on measured extinction values. Figure 10a shows the aerosol extinction kernels for the four SAGE II measurement wavelengths (386, 452, 525, and 1020 nm) assuming spherical particles composed of a mixture of sulfuric acid and water. Generally, aerosol extinction coefficient and particle size are positively correlated; that is, as aerosol extinction coefficient increases the mean particle size also increases. Thus, for low aerosol loading it is possible that a significant fraction of SAD lies at particle sizes to which visible wavelength aerosol extinction is almost totally insensitive and, as a result, the calculation of SAD is prone to substantial uncertainties. The retrieval of SAD for low aerosol loading is not necessarily biased to low values but rather it is highly dependent on how the retrieval process fills the small end of the particle size distribution and thus can be biased either high or low. This will be demonstrated later in this section. Many techniques have been applied to this calculation for SAGE II data, each of which filled this 'blind spot' in a somewhat

different manner (Wang et al., 1989; Thomason et al., 1997; Steele et al, 1997; Yue et al., 1999; Bingen et al., 2004). The operational SAD retrieval puts relatively little material at radii smaller than 50 nm and thus is likely to produce SAD values that are biased low to some degree (Thomason et al., 1997).

SAD is an important parameter in stratospheric chemistry and the low, effectively background aerosol levels currently observed establish a baseline for SAD effects. As a result, it is important to establish the level of reliability for SAGE II SAD estimates for use in chemical modeling. This is particularly important since SAGE II provides a unique global view of the aerosol burden from 1984 into 2005 spanning the entire Pinatubo period. The only other comparable data set is that provided by the Halogen Occultation Experiment (HALOE) which is also a space-based solar occultation experiment that operates in the infrared and produces SAD estimates that are in fact smaller than those estimated from SAGE II during background periods (Hervig et al, 1998, 2002). To quantify the range of possible solutions for SAD during background periods, we have developed simple models that allow us to put bounds on the maximum and minimum values for SAD that are consistent with the measured aerosol extinction and its wavelength dependence. As will be seen, these models are not terribly physical but the purpose of this exercise is to determine extreme limits on the SAD calculation and not to produce a new SAD retrieval algorithm. The family of existing, more physically-based retrievals would most likely show a smaller range of outcomes than those shown below.

For the first approach (Method 1), the minimum SAD value consistent with observed aerosol extinction is a straightforward calculation. It is based on the observation from Figure 11a that the Mie scattering efficiency monotonically increases for particle sizes between 0 and ~0.5 μm. As a result, on a per particle basis, the largest particles produce the most extinction at the cost of the smallest SAD. Thus the minimum possible SAD occurs for a monodispersed aerosol at the radius that preserves the observed extinction wavelength dependence modified by measurement uncertainty. For this model, aerosol extinction is given by

$$k(\lambda) - \varepsilon(\lambda) = N_{min} Q(r_{min}, \lambda) \pi r^2_{min}, \quad (2)$$

where $k$ and $\varepsilon$ are the aerosol extinction coefficient and it's associated uncertainty at wavelength $\lambda$, $N_{min}$ and $r_{min}$ are the number density and radius of the monodispersed aerosol, and $Q(r,\lambda)$ is the Mie extinction efficiency seen in Figure 10a. Figure 10b shows the 525 to 1020-nm extinction ratio to particle radius relationship for this model. This relationship is robust for particle sizes from 0 to 0.5 μm but becomes multi-valued at larger radii where the extinction ratio approaches 1. As a result, this method becomes ill-behaved for high aerosol loading periods (e.g., post-Pinatubo) and other situations where the measured extinction ratio is small. The minimum SAD, $SAD_{min}$, is computed by using the 525 to 1020-nm extinction ratio, $(k(525\ nm)-\varepsilon(525\ nm))/k(1020\ nm)$, to infer $r_{min}$ then $N_{min}$ is then computed using equation (2) above. Finally, $SAD_{min}$ is given by $4\pi N_{min} r^2_{min}$.

From a mathematical perspective, the maximum possible SAD that can be produced from SAGE II measurements is unbound. Since particles smaller than 0.1 μm are poor scatterers, it is possible to produce virtually unlimitedly large values of SAD by adding to the aerosol distribution derived for the minimum SAD (preserving the measured extinction coefficients) a second monodispersed mode at a very small radius (>>0.1 μm). For instance, using enough 10 nm particles to perturb the 525-nm aerosol extinction by the measurement uncertainty (~10%) produces SAD values in excess of $10^4$ $\mu m^2$ $cm^{-3}$ at the cost of a particle density on the order of $10^7$ $cm^{-3}$ for conditions where the operational method produces values on the order of 1 $\mu m^2$ $cm^{-3}$. Clearly, number densities of this order are physically unrealistic but this illustrates the scope of the mathematical freedom afforded in SAD calculations by visible near infrared wavelength extinction measurements.

An alternative approach to estimating a maximum value of SAD is based on the observation from in situ measurements that aerosol number density tends to be around 10 $cm^{-3}$ independent of the details of the size distribution [Deshler et al., 2003]. Starting with an alternate $SAD'_{min}$ computed using $k(\lambda)$ instead of $k(\lambda) - \varepsilon(\lambda)$ (with parameters $N'_{min}$ and $r'_{min}$) in Eq. 3, we compute a second monodispersed mode that brings the total number density to a fixed value ($N_{total}$ ~ 20 $cm^{-3}$) at a radius that perturbs the shortest

wavelength aerosol extinction wavelength used in the calculation by the measurement uncertainty ε(λ). In this case, $SAD_{max}$ (the Method 1 maximum) is given by

$$SAD_{\max} = SAD'_{\min} + 4(N_{total} - N_{\min})\pi r_{\max}^2 \quad (3)$$

where $r_{max}$ is the radius that is the solution to

$$\varepsilon(\lambda_{\min}) = Q(r_{\max}, \lambda_{\min})\pi r_{\max}^2 (N_{total} - N'_{\min}) \quad (4)$$

where ε is the uncertainty in the short wavelength aerosol extinction coefficient at wavelength $\lambda_{min}$ and. This method is appropriate for SAGE II data since the uncertainties at the short wavelength channels are much larger than those at 1020 nm and are highly correlated between channels. Unlike the minimum bound, this value is empirical and is not strictly a maximum bound to SAD and dependent on the a priori choice of $N_{total}$.

We have defined a more generalized form of the two monodispersed mode model which leaves the errors uncorrelated (Method 2) but leaves the total particle number, $N_{total}$, fixed at 20 $cm^{-3}$. In this approach, we compute a dense set of multi-wavelength aerosol extinction coefficient spectra that fills the bounds of bounds of three free parameters: $N_2$, the number of particles in the large mode which lies between 0 and 20. $cm^{-3}$, $r_s$, the radius of the small mode which lies between 0.01 and 0.5 μm, and $r_l$, the radius of the large mode which lies between 0.01 and 0.5 μm (and in practice greater than $r_s$). The maximum and minimum values for SAD occur where the computed extinction coefficients lay within the uncertainty bounds of the extinction coefficient measurements at two or more wavelengths ($SAD_{min2}$ and $SAD_{max2}$). We use a look up table with more than $10^7$ elements to determine a solution. While this approach is a 'brute force' approach, it avoids the numerical instability endemic to the direct retrieval process which is exacerbated by the fine structure in the extinction kernels and the use of monodispersed size distributions. The minimum and maximum SAD values that both Method 1 and Method 2 yield are intended to be extreme and the real distribution of particle sizes is likely to be spread across a broad range of particle sizes that yield SAD values well within the bounds derived here.

### 3.2 Examples of SAD Bound Calculations

Figure 11 shows the mean SAGE II aerosol extinction coefficient profiles for Northern midlatitudes in April 2001. This period occurs well within the current non-volcanic period and the profiles are typical of the period between 2000 and the end of the SAGE II measurement period in August 2005. Figure 12 shows a comparison of the Method 1 $SAD_{min}$ and $SAD_{max}$ values for this period along with the operational SAD profile. In this case, we show results for $N_{total}$ equal to 20 $cm^{-3}$ and using both the extinction at 452 and 525 nm as the short wavelength aerosol channel. As Figure 12 shows, we find that the SAD bounds are not strongly influenced by the choice of the 452 or 525 nm channels and we will limit further discussion to the use of the 525-nm channel. We also find that for these parameters that the difference between the minimum and maximum values of SAD increases from about a factor of 2 at 10 km to about a factor of 4 at 25 km and roughly follows the increase in the 525 to 1020-nm extinction coefficient ratio (decreasing mean particle size). The operational model tends to lie within these bounds where it runs from a little less than $SAD_{max}$ at 10 km to a little greater than $SAD_{min}$ at 25 km. In the main aerosol region below 25 km, the operational value lies around 30% of the way from $SAD_{min}$ to $SAD_{max}$ and thus follows the general expectation that it would tend produce surface area density values that are on the low end of the range of possible values.

Figure 13 shows the minimum and maximum SAD values for the 2 and 3-channel results for Method 2 compared to the operational results and Method 1 results. The 2 and 3-channel methods (using 525 and 1020 nm and 452, 525, and 1020 nm channels respectively) yield very similar results so we will restrict further discussion to the three channel method. Here, we find that the range in SAD is much larger than found for Method 1 and runs from a factor of 6 near 10 km to a factor of ~15 at 25 km. The preferred solutions for the minimum and maximum SADs for Method 2 follow a consistent pattern. For the minimum solution the solution uniformly occurs for the shallowest allowed slope in the extinction coefficient wavelength dependence (the largest allowed negative departures at the short wavelengths and largest allowed positive departures at the 1020 nm) whereas the maximum SAD solution invariably occurs for the steepest allowed solution (the largest allowed positive departures at the short wavelengths and largest allowed negative departures at the 1020 nm). We expect this result since the steeper slope implies smaller particles which require greater surface area to produce an

equivalent extinction as larger particles. This dependence is sufficiently non-linear that it overwhelms the relatively minor changes in the absolute magnitude of the extinction coefficients.

Figure 14 shows the derived free parameters ( $r_{min}$, $r_{max}$, $r'_{min}$, $N_{min,}$ and $N'_{min}$) for these solutions. We find that $r_{min}$ for the minimum and maximum SADs for Method 1 are essentially the same and the small particle size for the maximum SAD lies between 30 and 50 nm for most of the stratosphere. The large mode, $r_{lmax}$, for the maximum SAD in Method 2 is close to $r_{min}$ from Method 1 particularly above 15 km. On the other hand the small mode particle radius, $r_{smax}$, is larger than $r_{max}$ from Method 1 and varies from 60 to 100 nm in the stratosphere. For the minimum SAD for Method 2, $r_{smax}$ does not contribute significantly to the total surface area density but uniformly selects the smallest allowed particle size. As a result, the Method 2 approach effectively selects a single mode solution for minimum SAD and follows the argument made for the definition of the Method 1 minimum SAD. For both methods, the number density of the large mode for both the minimum and maximum SAD is less than 1 $cm^{-3}$ above 10 km and generally decreases with altitude. This result is consistent with past efforts to fit SAGE II extinctions with a priori size distribution models like the log-normal. In these efforts, the size distributions were commonly very narrow and the derived number densities were often much smaller than ~10 $cm^{-3}$ measured by in situ instruments (e.g., Wang et al., 1989).

Obviously, the dependence of the maximum SAD model on a priori parameters plays a role in understanding the upper limit of SAD that can be computed from SAGE II extinction coefficient measurements. For instance, doubling $N_{total}$ to 40 $cm^{-3}$ yields a 15 to 40% increase in both $SAD_{max}$ and $SAD_{min}$ for Method 1 depending on altitude. The dependence is not linear since the increase number density is in part compensated for by a reduction in the inferred particle size for the small mode aerosol. We find that including a third monodispersed mode never yields a significant third mode for either the minimum or maximum SAD. These results make us confident that two monodispersed modes are yielding the extreme results that we are seeking.

As an extension to this study, we have examined the impact of additional measurements on the range of surface area density possible from SAGE II measurements. In particular, we consider including a channel from the infrared where sulfate aerosol strongly absorbs. In the infrared, provided that the refractive index of the aerosol is well known, the aerosol extinction coefficient is roughly proportional to aerosol volume density for a broad range of aerosol sizes and, as a result insensitive to aerosol size. We have examined this effect using the SAGE II operational estimate of aerosol volume with an uncertainty of 15% as a stand in for an infrared measurement for use in along with the 3 visible channel version of Method 2. Clearly, the SAD values determined from this experiment cannot be taken at face value. Nonetheless, as shown in Fig. 15, the range of SAD is reduced to a factor between 1.5 and 2 through out the profile. From the values for $r_{lmax}$ and $r_{lmin}$ shown in Fig. 16, it is clear that the added information strongly limits the size of the large particle mode and they are very similar from 12 to 25 km. The addition of the volume estimate also has a significant impact on the $SAD_{min}$ calculation and the small mode is now a significant element in the surface area calculation. While this experiment should be interpreted cautiously, it is not difficult to conclude that a mix of visible and infrared aerosol measurements would be a much stronger measurement ensemble than either visible or infrared measurements alone.

### 3.3 Summary of Aerosol Surface Area Density Study

The SAD inferred from SAGE II visible and near-infrared aerosol extinction coefficient measurements is mathematically unbound however modest physically-based restrictions to the underlying particle number density reduces the range of SAD values for background periods to a factor or 2 to 15 depending on altitude and assumptions regarding the nature of the measurement uncertainty. It is important to remember that this range is the outcome of several unrealistic assumptions about the nature of the aerosol and the SAGE II measurements. However, this study helps to put a broad bracket around the range of SAD values that can be produced from SAGE II extinction coefficient measurements. Since Method 1 is the most realistic treatment of the SAGE II measurements, we believe that the maximum range of reasonable SAD values around the

current operational values is on the order of a factor of 2 for non-volcanic conditions. This factor is comparable to or greater than the differences found between the operational SAGE II SAD and SAD measurements made by in situ measurements such as the University of Wyoming Optical Particle Counter (e.g., Thomason and Peter 2006). The SAD model described above may not provide reasonable limits in regions in the stratosphere where strong particle nucleation occurs such as the lower tropical stratosphere [Brock et al., 1995] or the polar winter middle stratosphere [Deshler et al., 2003] since number densities may be considerably larger than those considered here though the SAGE II-measured extinctions remain valid. Also, it should also be noted that the relative difference between $SAD_{min}$ and $SAD_{max}$ becomes as small as 20% for higher aerosol loading.

## References


Anderson, S. M. and K. Mauersberger, Laser measurements of ozone absorption cross sections in the Chappuis band, Geophys. Res. Lett., 19, 933-936, 1992.

Anderson, S. M., J. Morton, and K. Mauersberger, Near-infrared absorption spectra of 16O3 and 18O3: Adiabatic energy of the 1A2 state, J. Chem. Phys., 93, 3826-3832, 1990.

Anderson, S. M., J. Maeder, and K. Mauersberger, Effect of isotopic substitution on the visible absorption spectrum of ozone, J. Chem. Phys., 94, 6351-6357, 1991.

Anderson, S. M., P. Hupalo, and K. Mauersberger, Rotational structure in the near-infrared absorption spectrum of ozone, J. Chem. Phys., 99, 737-739, 1993a.

Anderson, S. M., P. Hupalo, and K. Mauersberger, Ozone absorption cross section measurements in the Wulf bands, Geophys. Res. Lett., 20, 1579-1582, 1993b.

Bingen, C., D. Fussen and F. Vanhellemont, A global climatology of stratospheric aerosol size distribution parameters derived from SAGE II data over the period 1984-2000: 2. Reference data, *J. Geophys. Res., 109*, D06202, doi:10.1029 /2003JD003511, 2004b.

Brock, C. A., P. Hamill, J. C. Wilson, H. H. Jonsson and K. R. Chan, Particle formation in the upper tropical troposphere: A source of nuclei for the stratospheric aerosol, *Science 270*, 1650-1653, 1995.

Burkholder, J. B., and R. K. Talukdar, Temperature dependence of the ozone absorption spectrum over the wavelength range 410 to 760 nm, Geophys. Res. Lett., 21, 581-584, 1994.

Deshler, T., M. E. Hervig, D. J. Hofmann, J. M. Rosen and J. B. Liley, Thirty years of in situ stratospheric aerosol size distribution measurements from Laramie, Wyoming (41°N) using balloon-borne instruments, *J. Geophys. Res., 108*, 4167, doi:10.1029/2002JD002514, 2003.

Hervig, M. E., and T. Deshler, Evaluation of aerosol measurements from SAGE II, HALOE, and balloonborne optical particle counters, *J. Geophys. Res., 107* (D3), 10.1029/2001JD 000703, 2002.

Hervig, M. E., T. Deshler and J. M. Russell III, Aerosol size distributions obtained from HALOE spectral extinction measurements, *J. Geophys. Res., 103*, 1573-1583, 1998.

Hofmann, D. J., and J. M. Rosen, Antarctic observations of stratospheric aerosol and high altitude condensation nuclei following the El Chichon eruption, *Geophys. Res. Lett., 12*, 13-16, 1985.

McCormick, M. P., L. W. Thomason, and C. R. Trepte, Atmospheric effects of the Mount Pinatubo eruption, Nature, 373, 399-404, 1995.

Pitts, M. C., and L. W. Thomason, The impact of the eruptions of Mount Pinatubo and Cerro Hudson on Antarctic aerosol levels during the 1991 austral spring, Geophys. Res. Lett., 20, 2451, 1993.

Randel, W.J., F. Wu and D. Gaffen, Interannual variability of the tropical tropopause derived from radiosonde data and NCEP reanalyses. J. Geophys. Res., 105, 15509-15523, 2000.

Russell, P. B., J. M. Livingston, R. F. Pueschel, J. J. Hughes, J. B. Pollack, S. L. Brooks, P. Hamil, L. W. Thomason, L. L. Stowe, T. Deshler, E. G. Dutton, and R. W. Berstrom, Global to microscale evolution of the Pinatubo volcanic aerosol, derived from diverse measurements and analyses, J. Geophys. Res. 101, 18745-18764, 1996.

Shettle, E. P. and S. M. Anderson, New Visible and Near IR Ozone Cross Sections for MODTRAN, presented at the 17th Annual Review Conference on Atmospheric Transmission Models, Phillips Laboratory, Bedford, MA, 7-8 June 1994.

Steele, H. M., and P. Hamill, Effects of temperature and humidity on the growth and optical properties of sulfuric acid-water droplets in the stratosphere, *J. Aerosol Sci.*, *12*, 517-528, 1981.

Steele, H. M., and R. P. Turco, Retrieval of aerosol size distributions from satellite extinction spectra using constrained linear inversion, *J. Geophys. Res., 102,* 16737-16747, 1997.

Thomason, L. W., G. S. Kent, C. R. Trepte and L. R. Poole, A comparison of the stratospheric aerosol background periods of 1979 and 1989-1991, *J. Geophys. Res., 102*, 3611-3616, 1997a.

Thomason, L. W., L. R. Poole and T. R. Deshler, A global climatology of stratospheric aerosol surface area density as deduced from SAGE II: 1984-1994, *J. Geophys. Res., 102,* 8967-8976, 1997b.

Thomason, L. W. and T. Peter,

Trepte, C. R., L. W. Thomason, and G. S. Kent, 1994: Banded structures in stratospheric aerosol distributions, Geophys. Res. Lett., 22, 2397-2400, 1994.

Wang, P. H., M. P. McCormick, L. R. McMaster, W. P. Chu, T. J. Swissler, M. T. Osborn, P. B. Russell, V. R. Oberbeck, J. Livingston, J. M. Rosen, D. J. Hofmann, G. W. Grams, W. H. Fuller and G. K. Yue, SAGE II aerosol data validation based on retrieved aerosol model size distribution from SAGE II aerosol measurements, *J. Geophys. Res., 94*, 8381-8393, 1989.

Wang H. J., D. M. Cunnold, L. W. Thomason, J. M. Zawodny, and G. E. Bodeker, Assessment of SAGE version 6.1 ozone data quality, J. Geophys. Res., 107 (D23), 4691, doi:10.1029/2002JD002418, 2002.

Yue, G. K., A new approach to retrieval of aerosol size distributions and integral properties from SAGE II aerosol extinction spectra, *J. Geophys. Res., 104,* 27491-27506, 1999.

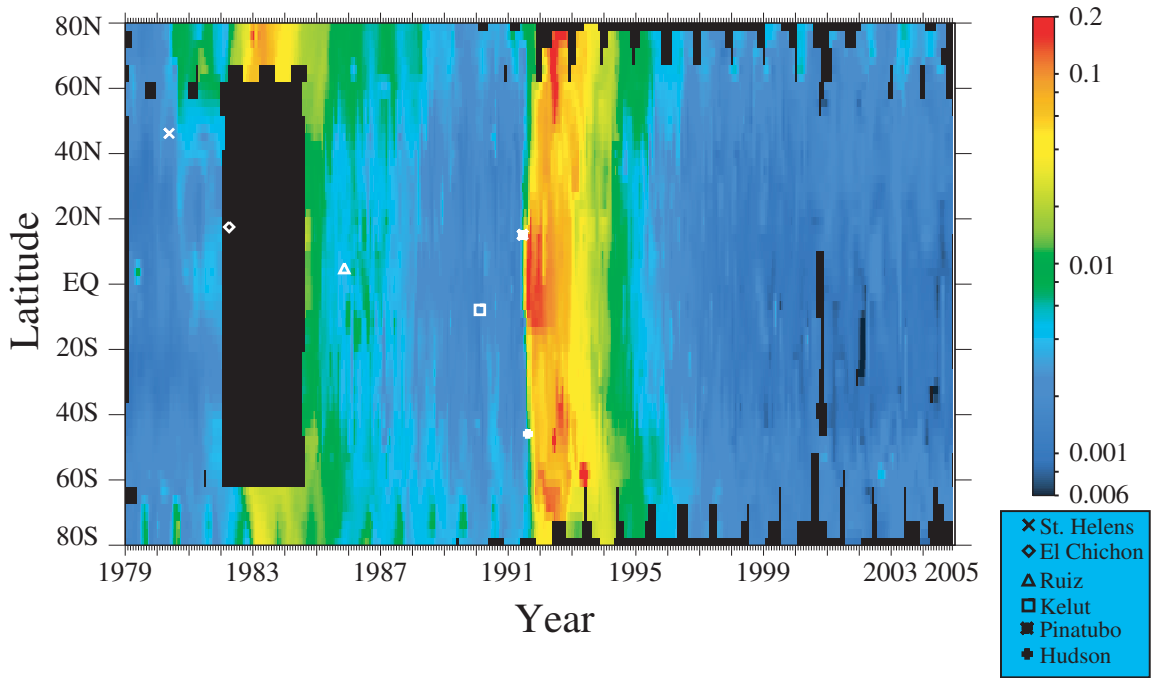


Figure 1. This figure depicts the 1020-nm stratospheric optical depth from SAM II, SAGE, SAGE II and SAGE III for the period from January 1979 through the end of 2004. Between the eruption Pinatubo in June 1991 and mid 1993, aerosol extinction coefficient profiles are supplemented by lidar data following the method described in Thomason and Peter [2006].

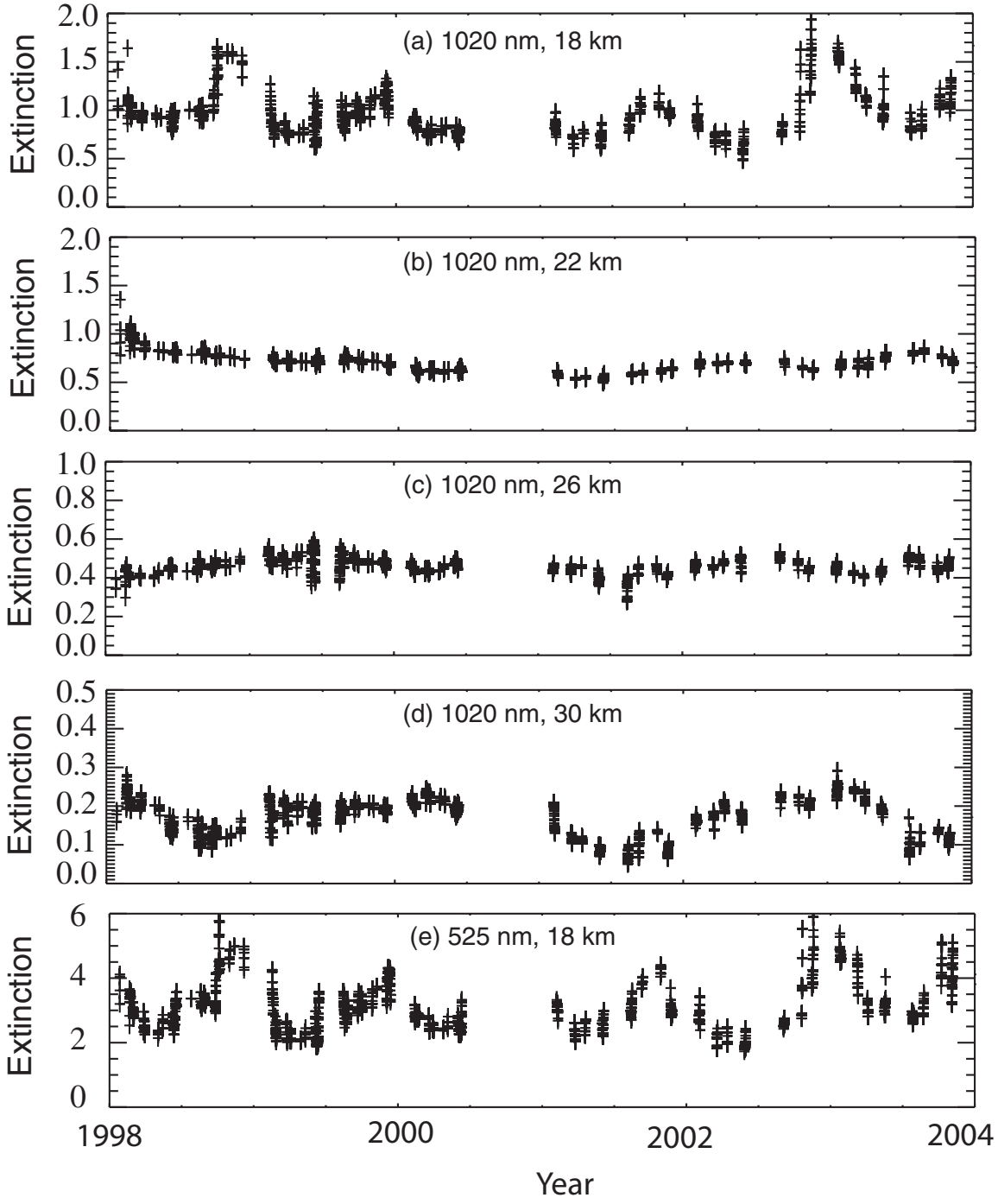


Figure 2. This figure depicts SAGE II stratospheric 1020-nm aerosol extinction coefficient variability (in units of 1/km) for altitudes of 18 (a), 22 (b), 26 (c) and 30 km (d) between 10°N and 10°S for the years 2000 through 2005. In addition, 525-nm aerosol extinction variability at 525 nm is shown in frame e. The effects of the eruptions of Ruang and Reventador in late 2002 can be seen at 18 km.

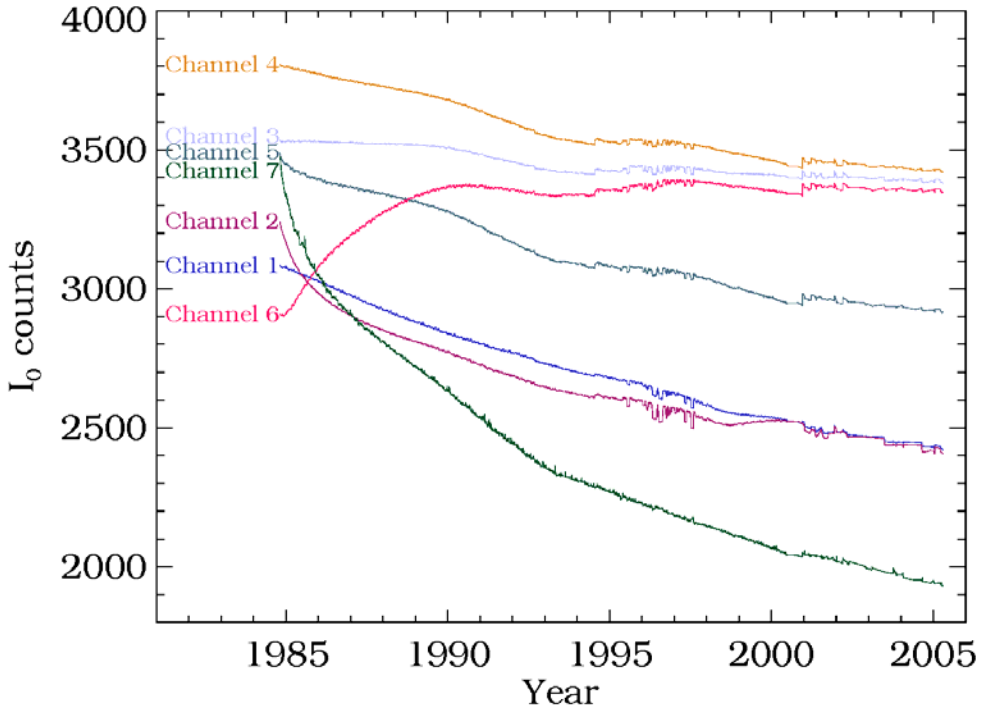


Figure 3. A depiction of SAGE II exoatmospheric counts for channels 1 through 7 through the lifetime of the instrument. The channels have central wavelengths of 1020, 940, 600, 525, 453, 448, and 386 nm, respectively.

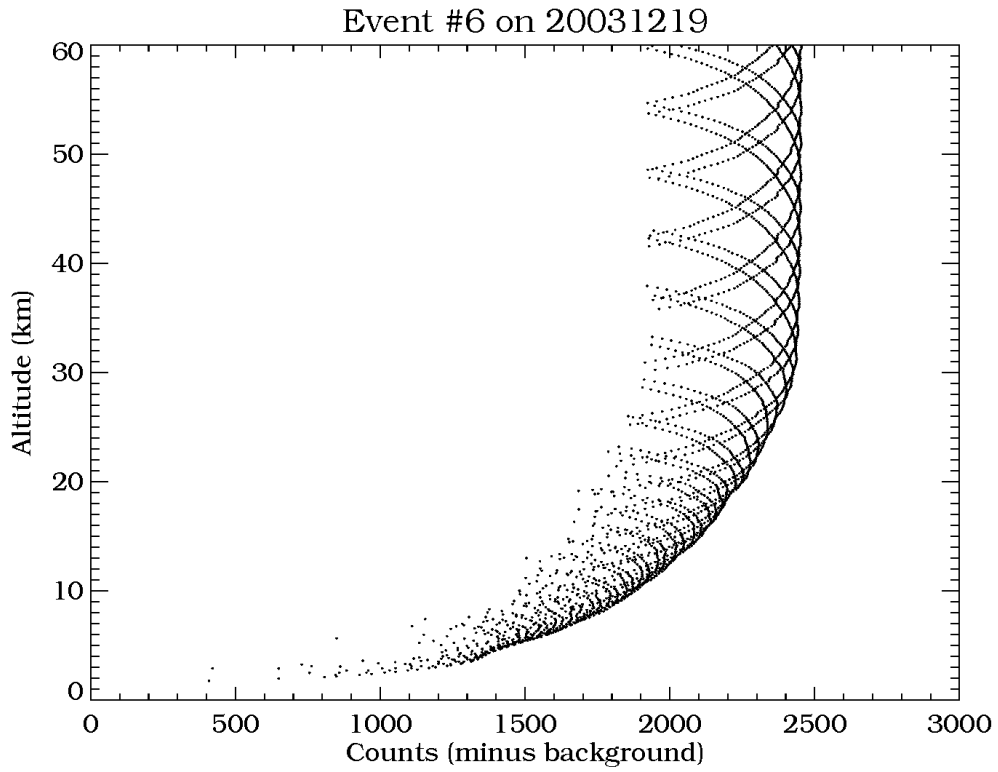


Figure 4. Shows the instrument counts, minus background, for the center 90% of the sun, as a function of altitude, for an event which occurred on December 19, 2003 at 21.1º N, 142.0º E.

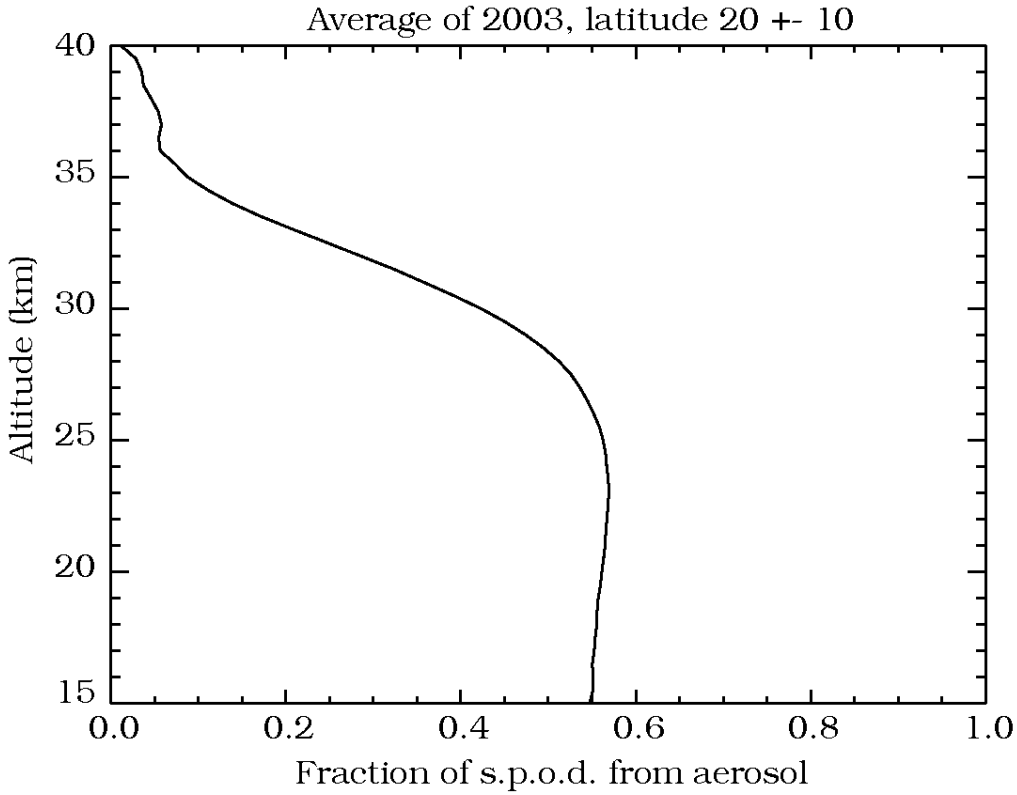


Figure 5. This figure shows the fraction of the slant path optical depth in the 1020 nm channel that is attributable to aerosol. All events between 10ºN and 30ºN in 2003 are included in the average shown here.

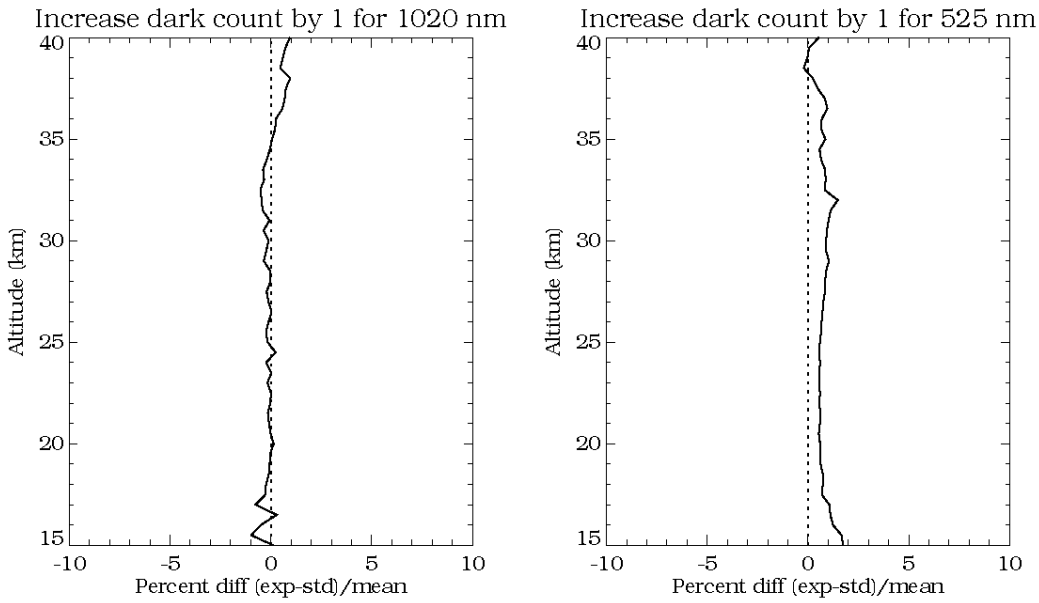


Figure 6. These figures show the effect on the ratio of 525 nm to 1020 nm aerosol extinction of increasing the number of counts subtracted from the signal to correct for "dark current". The plot shows the percent difference of the means of multiple processed events, with the sense (exp-std)/mean*100% where "std" and "exp" refer to the assumed-correct subtraction and the perturbed subtraction, respectively, and "mean" is (std+exp)/2. The events included are those between 10ºN and 30ºN latitude in the year from October 2001 to September 2002. The left panel shows the result when the experimental perturbation is made to the 1020 nm channel, while the right shows the effect of perturbing the 525 nm channel.

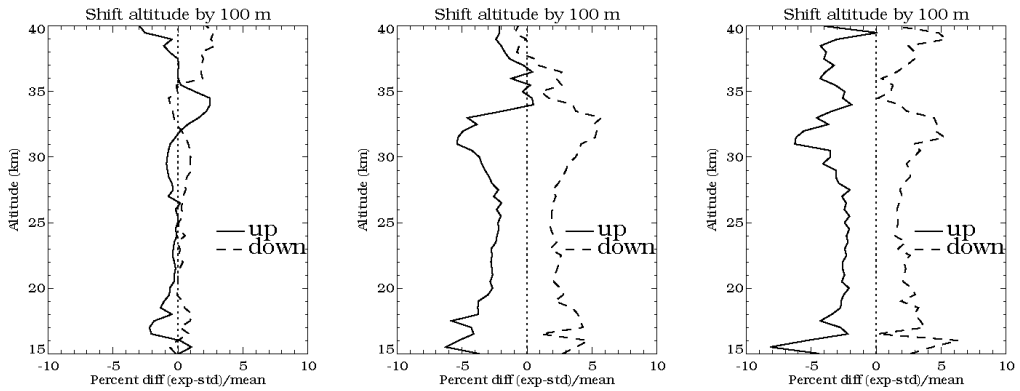


Figure 7. This figure shows the effect of a shift in the altitude registration upward (solid lines) or downward (dashed). The difference between shifted and unshifted aerosol extinctions are shown in percent for 1020-nm aerosol extinction (left), 525-nm aerosol extinction (middle) and the ratio of 525-nm/1020-nm extinction (right). The sense of the percent difference is ("experimental"-"standard")/"mean" where "experimental" is the mean of all the perturbed measurements, "standard" is the mean of unperturbed measurements and "mean" is ("experimental"+"standard")/2. The measurements represented here are all of the events between 10ºN and 30ºN for the year from October 2001 to September 2002. Measurements at levels that appear to have been contaminated by clouds have been removed.

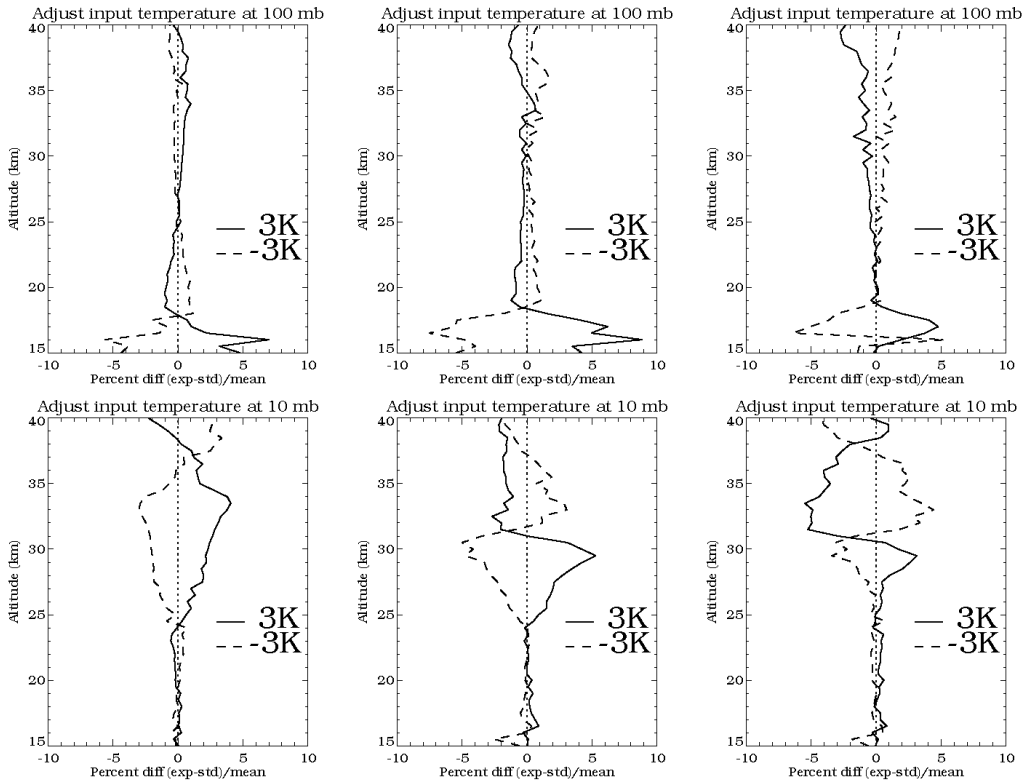


Figure 8. Upper panels show the result of perturbing the input temperature value at 100 mb by 3K (solid lines) and -3K (dashed). Percent differences for the 1020-nm extinction (left), 525-nm extinction (middle) and 525-nm/1020-nm ratio (right) are ("experimental" - "standard")/"mean" with the meanings as in Figure 6. The suite of measurements is also the same as in Figure 6, and the cloud clearing is the same. The lower panels show the results for a perturbation to the input temperature at the 10 mb level.

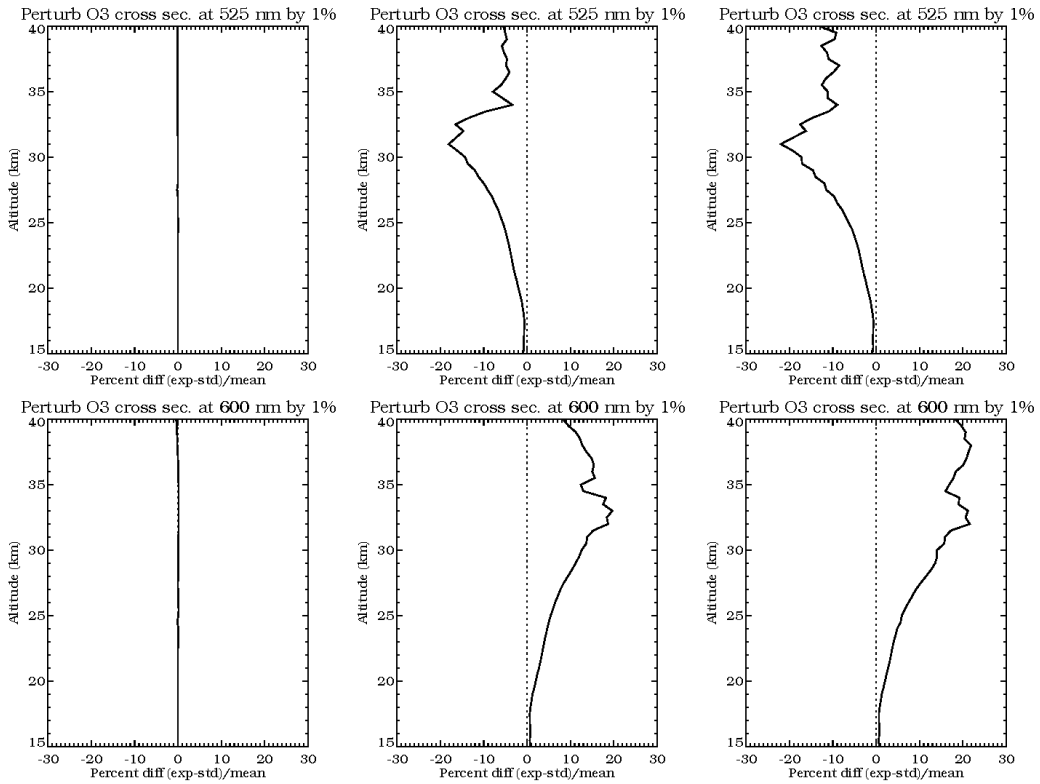


Figure 9. This figure shows the effect of perturbing the ozone cross section at 525 nm (top) and separately at 600 nm (bottom) by 1%. The effects on the 1020-nm aerosol extinction measurement (left), 525-nm aerosol extinction measurement (middle) and the ratio (right) are shown. Details of the experiments are otherwise the same as Figures 6, 7, 8, and 9. Note the range of the abscissa has been increased on these plots compared to previous figures.

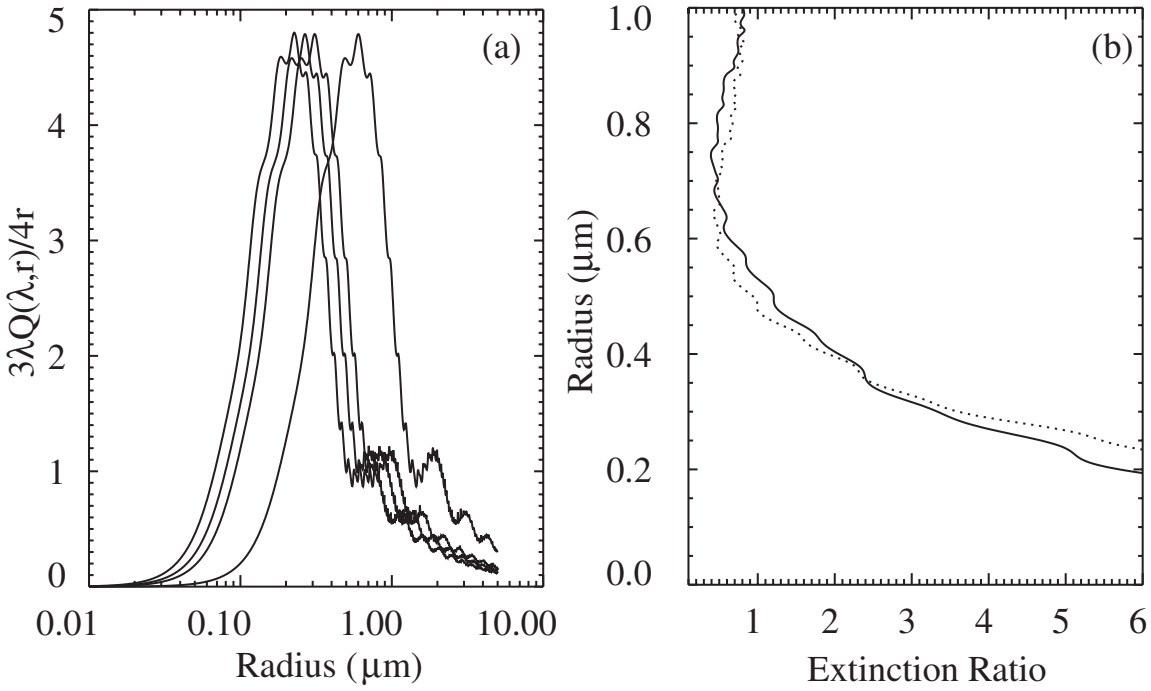


Figure 10. (a) Extinction kernels for SAGE II aerosol extinction channels at 385(left-most), 452, 525, and 1020 nm (right-most) for spherical water/sulfuric acid drops at stratospheric temperatures. (b) Particle radius as a function of the 525-nm channel to the 1020-nm extinction kernel ratio (or extinction coefficient ratio for a monodispersed aerosol).

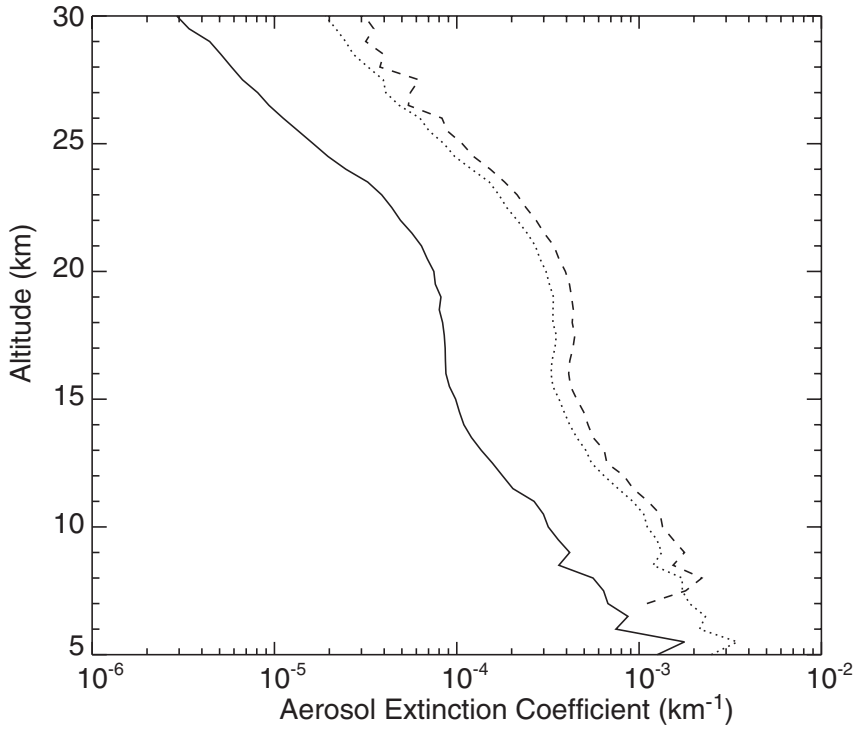


Figure 11. Mean Northern midlatitude SAGE II aerosol extinction coefficient profiles for April 2001 for 1020 (solid), 525 (dotted), and 452 nm (dashed).

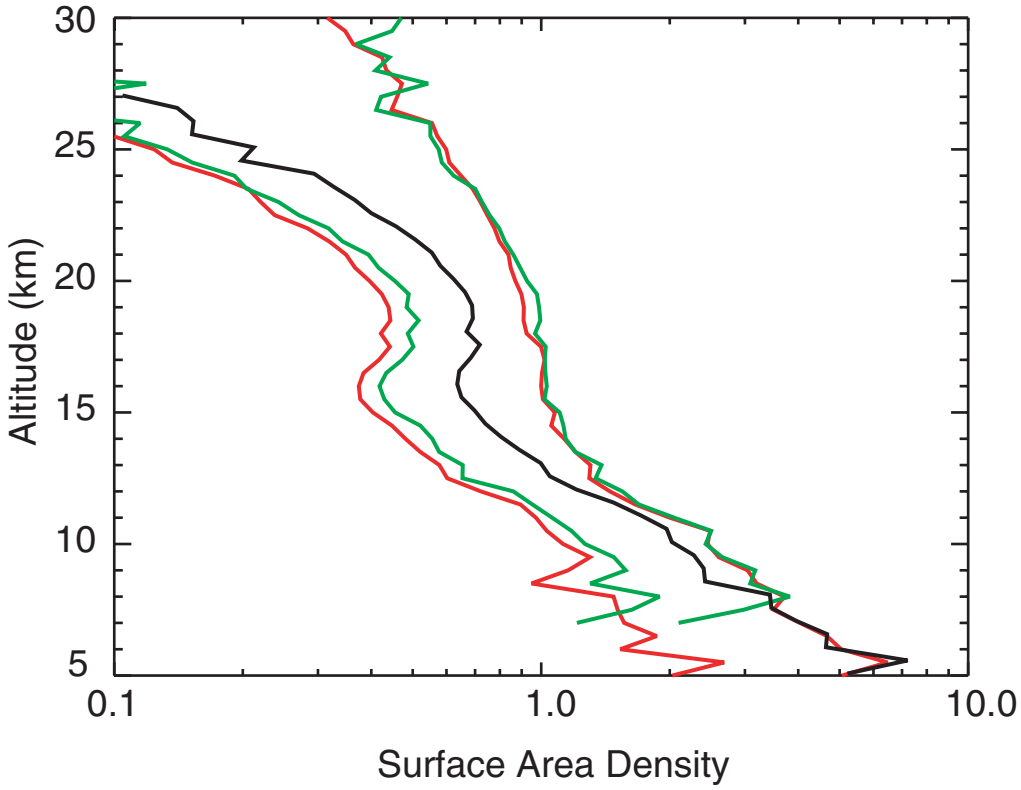


Figure 12. This figure shows a comparison of the operational SAGE II SAD (black) and the SAD computed using Method 1 and 525-nm (red) and 452-nm (green) as the low wavelength aerosol extinction coefficient channel.

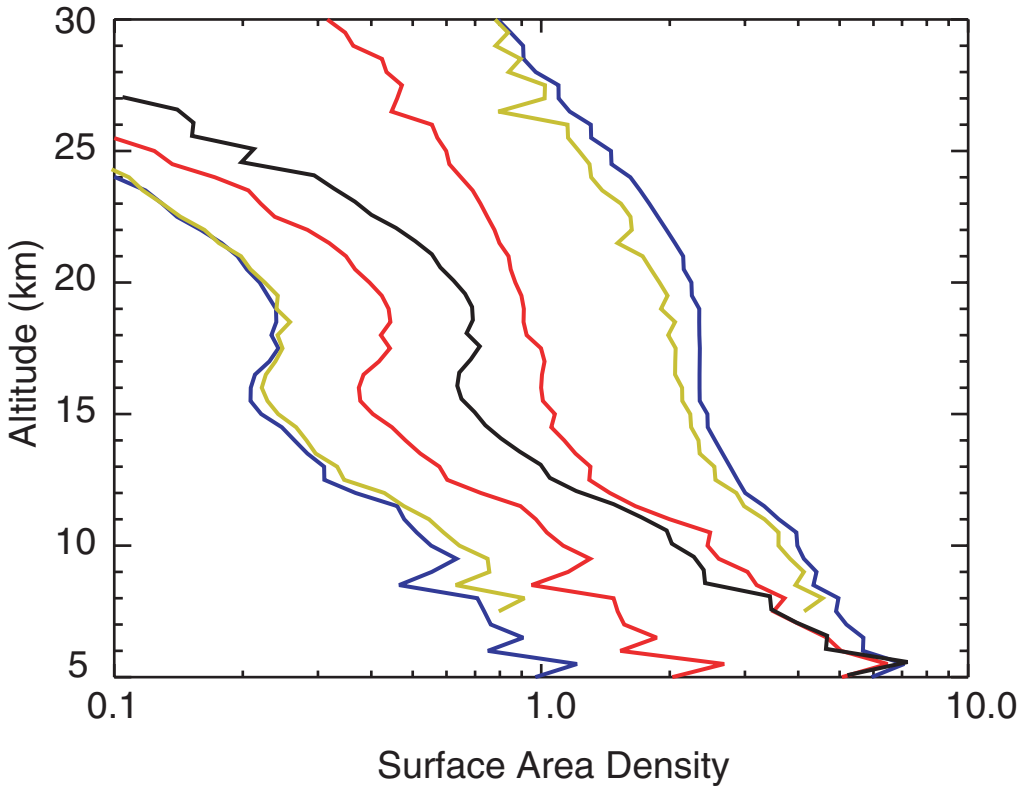


Figure 13. This figure shows the comparison of operational SAGE II SAD with the Method 1 minimum and maximum SAD using 525-nm aerosol extinction coefficient (red) and the minimum and maximum Method 2 SAD using 2 channels at 525 and 1020 nm channels (blue) and 3 channels at 452, 525, and 1020 nm (gold).

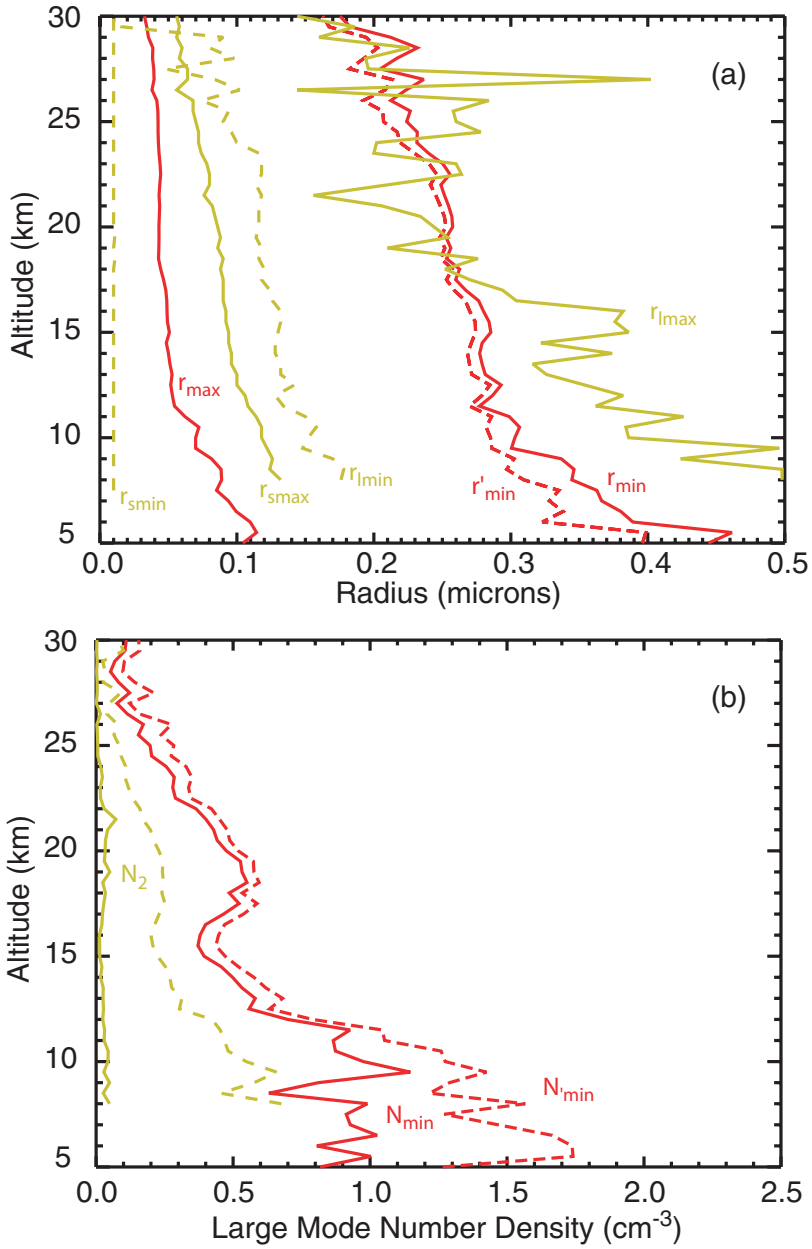


Figure 14. This figure shows the profiles of the Method 1 dependent parameters $r_{min}$, $r_{max}$, and $r'_{min}$ (on frame a) and $N_{min}$ and $N'_{min}$ (b) in red. In addition, it shows Method 2 free parameters $r_{lmax}$, $r_{lmin}$, $r_{smax}$, and $r_{smin}$ (a) and N2 for the maximum SAD (solid) and for the minimum SAD (dashed) in gold.

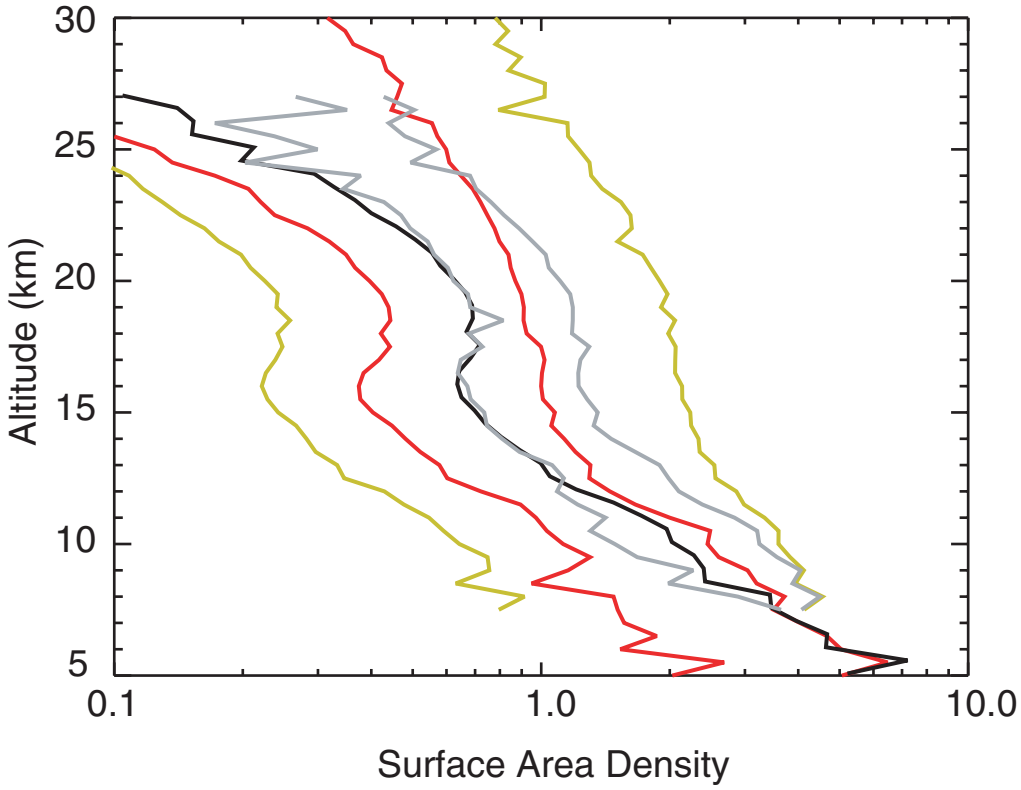


Figure 15. This figure shows the comparison of operational SAGE II SAD with the Method 1 SAD using 525-nm aerosol extinction coefficient (red) and the Method 2 SAD using the 525 and 1020 nm channels (blue) and the Method 2 SAD computed using the channels at 525 and 1020 nm plus a pseudo-infrared channel (cyan).

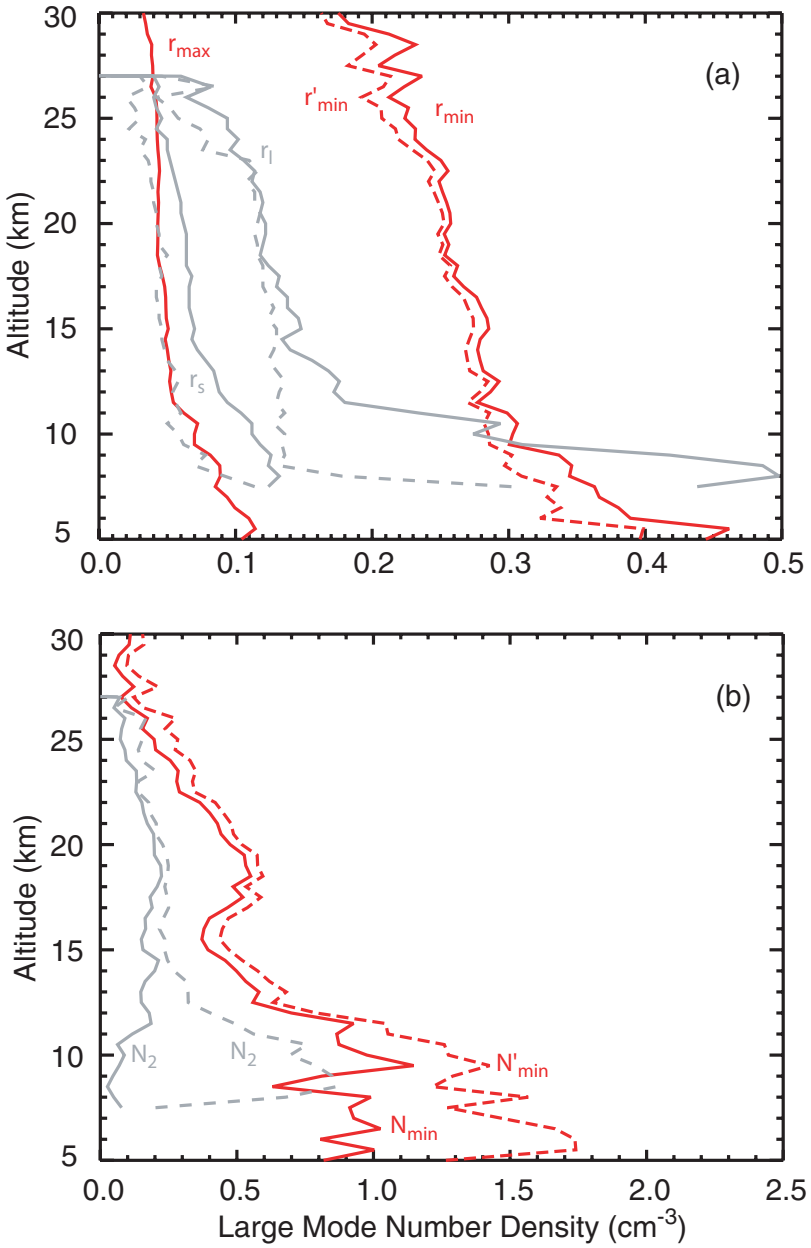


Figure 16. This figure shows the profiles of the Method 1 dependent parameters $r_{min}$, $r_{max}$, and $r'_{min}$ (on frame a) and $N_{min}$ and $N'_{min}$ (b) in red. In addition, it shows Method 2 for 3 channels plus a pseudo-infrared channel channels and a free parameters $r_{lmax}$, $r_{lmin}$, $r_{smax}$, and $r_{smin}$ (a) and $N_2$ for the maximum SAD (solid) and for the minimum SAD (dashed) in cyan (b).